THE JOURNAL OF PHYSICAL CHEMISTRY C

Feature Article

pubs.acs.org/JPCC

Recent Developments in Shape-Controlled Synthesis of Silver Nanocrystals

Xiaohu Xia,[†] Jie Zeng,[‡] Qiang Zhang,[§] Christine H. Moran,[†] and Younan Xia*[,†]

[†]The Wallace H. Coulter Department of Biomedical Engineering, Georgia Institute of Technology and Emory University, and School of Chemistry & Biochemistry and School of Chemical & Biomolecular Engineering, Georgia Institute of Technology, Atlanta, Georgia 30332, United States

[‡]Hefei National Laboratory for Physical Sciences at the Microscale, and Department of Chemical Physics, University of Science and Technology of China, Hefei, Anhui 230026, P. R. China

[§]School of Life Science, East China Normal University, Shanghai 200241, P. R. China

ABSTRACT: This feature article introduces our recent work on understanding the roles played by citrate and poly(vinyl pyrrolidone) (PVP) as capping agents in seed-mediated syntheses of Ag nanocrystals with controlled shapes. We have demonstrated that citrate and PVP selectively bind to Ag(111) and Ag(100) surfaces, respectively, and thus favor the formation of Ag nanocrystals enclosed preferentially by {111} or {100} facets. In addition, we have quantified the coverage density of PVP adsorbed on the surface of Ag nanocubes. On the basis of the mechanistic understanding, a series of Ag nanocrystals with controlled shapes and sizes have been successfully synthesized by using different combinations of seeds and capping agents: single-crystal spherical/cubic seeds with citrate for cuboctahedrons and octahedrons or with PVP for cubes and bars and plate-like seeds with citrate for enlarged thin plates or with PVP for thickened plates.

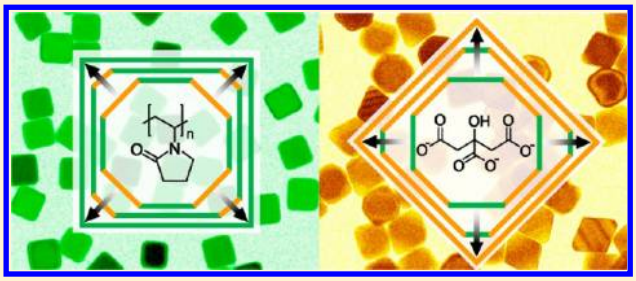

INTRODUCTION

It is well-established that the shape of Ag nanocrystals plays an important role in determining their physical and chemical properties,[1−9] including localized surface plasmon resonance (LSPR) and surface-enhanced Raman scattering (SERS). Over the past decade, Ag nanocrystals with a myriad of shapes (e.g., spheres, cubes, octahedrons, right bipyramids, bars, plates, rods, and wires) have been synthesized using various methods.[10−16] Among these methods, facet-specific capping has emerged as a facile and effective route to the synthesis of Ag nanocrystals with controlled shapes. The concept of facet-specific capping can probably find its root in heterogeneous catalysis, where chemisorption of atomic or molecular species from the gas phase often results in drastic changes to the shape or morphology of metal nanoparticles.[17−19] For example, Harris reported that spherical Pt nanoparticles were transformed into nanocubes when the sample was exposed to H_2 gas containing a trace amount of H_2S.[20] It was proposed that the {100} facets were preferentially formed over other types of facets in the presence of H_2S due to a stronger interaction of sulfur with the Pt(100) surface.

In solution-phase syntheses of nanocrystals, facet-specific capping can also have a profound impact on the shape evolution of seeds during growth. In principle, the use of a capping agent controls the morphology of a nanocrystal thermodynamically because it reduces the surface free energy (γ) of a specific type of facet through chemisorption. Defined as the excess free energy per unit area for a particular facet,[21,22] the surface free energy plays a crucial role in understanding and predicting the growth habit of a seed and thus the shape/morphology taken by the final product. When a reaction is under thermodynamic control, the growth of a nanocrystal will proceed along the path that minimizes the total surface free energy of the system.[23,24] For Ag nanocrystals, in the absence of capping agents, the surface free energies of low-index facets increase in the following order: $\gamma_{\{111\}} < \gamma_{\{100\}} < \gamma_{\{110\}}$.[24,25] When Ag nanocubes enclosed by {100} facets are employed as seeds for growth, the {100} facets will gradually be replaced with the more stable {111} facets, leading to the formation of truncated cubes, cuboctahedrons, and finally octahedrons.[14,26,27] It is worth emphasizing that the surface free energies of various facets can be reduced due to the selective binding or chemisorption of a capping agent. For example, it has been shown that poly(vinyl pyrrolidone) (PVP) can selectively bind to Ag(100) to make its surface free energy lower than that of Ag(111), resulting in the formation of nanocubes and nanobars enclosed by the otherwise less stable {100} facets.[28,29] Citrate, in contrast, has been shown to bind more strongly to Ag(111) than Ag(100), favoring the formation of nanoparticles with {111} facets displayed on the surface.[11,30] In principle, the facets exposed on the surface of a final product should be a manifestation of the order of free energies for different facets

Received: June 20, 2012
Revised: August 20, 2012
Published: September 4, 2012

   dx.doi.org/10.1021/jp306063p | J. Phys. Chem. C 2012, 116, 21647−21656

after the chemisorption of a capping agent has been taken into consideration.

The preferential binding of citrate and PVP to Ag(111) and Ag(100), respectively, can be ascribed to their unique molecular structures and conformations (Figure 1). Computational

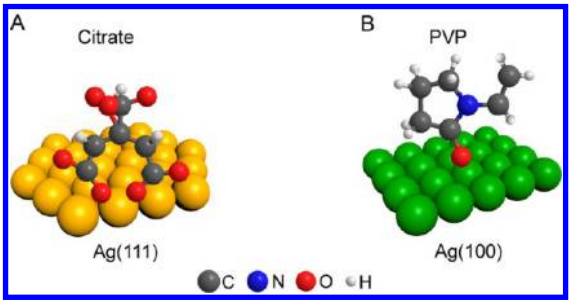

Figure 1. Schematic illustrations of (A) a citrate group bound to the Ag(111) surface and (B) a repeating unit of PVP bound to the Ag(100) surface. The Ag atoms on the (111) and (100) surfaces are shown as yellow and green spheres, respectively.

studies based on the density functional theory (DFT) indicated that the binding energies of the citrate group to Ag(111) and Ag(100) surfaces were 13.84 and 3.69 kcal/mol, respectively.[31] On the basis of the Boltzmann distribution, this huge difference (ΔE = 10.15 kcal/mol) in binding energies corresponds to a difference of six orders in magnitude for the binding constants to Ag(111) and Ag(100) surfaces. Such a difference in binding energies can be correlated to the degree of match or mismatch in geometry/symmetry between the molecule and the Ag surface. A good match in geometry between citrate and the Ag(111) surface generates four ligand–surface bonds (Figure 1A), while only two bonds are formed with Ag(100).[31] In comparison with small molecules such as citrate, the analysis of PVP, a polymeric capping agent, is much more complicated due to the involvement of polyvalency. According to experimental studies using various spectroscopic techniques, it is believed that PVP can bind to the Ag(100) surface through the oxygen and possibly the nitrogen atoms in the 2-pyrrolidone ring (Figure 1B).[32−36] A recent study based on density functional theory (DFT) calculations at both the segment and chain levels confirmed that PVP bound more strongly to the Ag(100) surface than Ag(111).[37] It was revealed that the probability of binding to Ag(100) increased exponentially with the number of repeating units but did not seem to depend on the conformations of the polymer since there were many different configurations that PVP could take with respect to the surface.

These computational calculations have greatly advanced our fundamental understanding of the interaction between a capping agent and a Ag surface at the atomic scale and thus helped gain insight into the specific roles played by citrate and PVP. Although implementing them into practical syntheses remains to be a challenge, significant process has been made in recent years. In this feature article, we will focus on the experimental approaches we have taken to understand the roles played by citrate and PVP and how they can be employed to direct the evolution of Ag nanocrystals into different shapes. To simplify the reaction parameters and thereby better understand the role played by a capping agent, all the experiments were conducted using seed-mediated growth. As a major advantage over other methods based on homogeneous nucleation, seed-mediated growth allows us to concentrate on the growth step by disentangling the complex nucleation steps, making it much easier to design the synthesis for a desired product.[38−43]

The article is organized as follows: First, we describe a model system involving the use of Ag nanospheres and citrate/PVP as the seeds and capping agents, respectively, to single out the role played by citrate/PVP. We then extend the strategy of facet-specific capping to platelike Ag seeds. In the following two sections, we provide a quantitative analysis of PVP adsorption on the Ag(100) surface and then specifically discuss the synthesis of Ag nanocrystals enclosed by high-index facets. Finally, we briefly discuss the investigation of shape- and size-dependent LSPR properties of Ag nanocrystals.

CITRATE VS PVP IN CONTROLLING THE SHAPE OF AG NANOCRYSTALS

Although our early work has demonstrated the preferential binding of citrate to Ag(111) and PVP to Ag(100), it should be pointed out that the explicit role played by either citrate or PVP in controlling the shape of Ag nanocrystals was not deciphered until recently. This was because none of these experiments was conducted under the same reaction conditions, and it was impossible to rule out the possible influences of other parameters. To address this issue, we designed a set of experiments based on seed-mediated growth to single out the roles played by citrate and PVP in the evolution of different shapes for Ag nanocrystals.[44] The experiments were conducted under identical reaction conditions except for the use of citrate or PVP as the capping agent (see Figure 2A for a schematic).

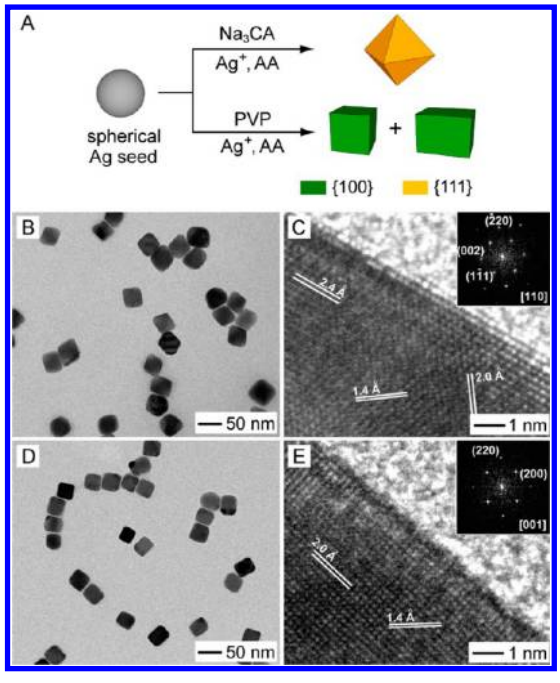

Figure 2. (A) Schematic showing the growth of a spherical Ag seed in the presence of citrate or PVP as the capping agent. (B) TEM and (C) HRTEM images of Ag octahedrons obtained by adding $AgNO_3$ into an aqueous suspension of spherical Ag seeds, together with ascorbic acid (AA) and sodium citrate (Na_3CA). (D) TEM and (E) HRTEM images of Ag cubes and short bars prepared under the same conditions as in (B) except that PVP, instead of Na_3CA, was added as the capping agent. The insets in (C) and (E) are the selected area electron diffraction (SAED) patterns taken from the same particles as shown in (C) and (E), respectively. (Adapted with permission from ref 44, copyright 2010 American Chemical Society).

Specifically, the syntheses involved the use of Ag nanospheres (with an average diameter of 28 nm) as the seeds in an aqueous system, with L-ascorbic acid (AA), $AgNO_3$, and citrate or PVP serving as the reductant, precursor, and capping agent, respectively. The spherical Ag seeds were prepared by quenching a polyol synthesis with an ice–water bath at 10 min into the reaction according to our previously reported procedure.[44] When sufficient $AgNO_3$ was introduced into the reaction solution in the presence of citrate as a capping agent, we obtained Ag octahedrons of 40 nm in edge length (Figure 2B). By substituting citrate with PVP, however, the same spherical seeds ultimately grew into a mixture of nanocubes (25%) and slightly elongated nanocubes or nanobars (75%, see Figure 2D).

Note that the surface of a spherical Ag seed actually contains a mixture of {111} and {100} facets in roughly equal proportion. It was suggested by the high-resolution transmission electron microscopy (HRTEM) images (Figure 2, C and E) that in the presence of citrate the final products (i.e., octahedrons) were dominated by {111} facets, and the {100} facets had all disappeared. In the presence of PVP, however, the final products (i.e., nanocubes and nanobars) were dominated by {100} facets, and the {111} facets had all disappeared. The selective binding of citrate to Ag{111} facets makes these facets more stable than {100} facets. The addition of Ag atoms therefore only occurred on {100} facets, resulting in gradual shrinkage of {100} facets during growth and eventually the formation of Ag octahedrons entirely enclosed by {111} facets. When PVP was present, {100} facets were expected to be more stable and thus grew more slowly than {111} facets. In this case, the total area of {100} facets was constantly enlarged at the expense of {111} facets during growth, leading to the evolution from spherical seeds to nanocubes and nanobars enclosed by {100} facets. It is worth pointing out that the formation of Ag octahedrons experienced an intermediate stage that contained a mixture of cuboctahedrons and truncated octahedrons. Both of these intermediates had an increased ratio of {111} to {100} on the surface compared to the starting seeds, but the supply of Ag atoms was insufficient for the seeds to fully develop into octahedrons. We also conducted another experiment for the citrate-mediated synthesis by replacing the spherical seeds with cubic Ag seeds, while all the other parameters were kept the same. As expected, octahedrons were still obtained despite a larger proportion of {100} facets on the cubic than the spherical seeds. This observation provides additional evidence to support our proposed growth mechanism based on surface capping.

This study directly compared the roles of capping agents in controlling the evolution of shape for Ag nanocrystals during seed-mediated growth. Briefly, citrate can selectively bind to {111} facets and thus drive the deposition of Ag atoms onto other facets, resulting in the formation of Ag nanocrystals (e.g., octahedrons) encased by {111} facets. Unlike citrate, PVP binds more strongly to {100} than other facets, leading to the formation of Ag nanocrystals (e.g., nanocubes and nanobars) enclosed by {100} facets only. In a sense, the growth of a Ag seed and thus the shape or morphology of the final product was predictable if citrate or PVP was known to be present as a capping agent.

EXTENDING THE CAPPING STRATEGY TO PLATELIKE SEEDS

Silver nanoplates offer a class of interesting nanostructures for investigating the role of twin defects or stacking faults in controlling the evolution of shape. Mirkin et al. first reported a photoinduced method in 2001 for the generation of Ag nanoplates with high yields.[11] Since this pioneering work, a rich variety of synthetic routes have been reported for producing plate-like Ag nanostructures.[45−50] It is well-known that Ag nanoplates are covered by {111} facets on both the top and bottom surfaces, together with twin planes and stacking faults on the side faces parallel to the lateral plane.[11,46] Despite the availability of many different methods for the syntheses of Ag nanoplates, most of them only allow for lateral growth along the twin defects and stacking faults, resulting in the formation of large, thin plates. There was no demonstration of vertical growth that would greatly increase the thickness of Ag nanoplates.

We recently extended the use of citrate and PVP as capping agents to the growth of platelike Ag seeds.[51] Figure 3A schematically illustrates the two situations for epitaxial growth of Ag on platelike Ag seeds in the presence of citrate and PVP as the capping agents, respectively. If citrate and PVP acted in similar manners as were observed in the growth of spherical Ag seeds, the presence of citrate and PVP should increase the area of Ag(111) and Ag(100) surfaces on the Ag nanoplates, respectively. In other words, the epitaxial growth of Ag on a platelike seed could be directed to preferentially occur in the lateral or vertical direction by using citrate or PVP as the capping agent.

Experimentally, we employed triangular Ag plates 45 nm in edge length and 5 nm in thickness as the seeds, which were prepared using a previously reported, seed-mediated protocol, and their structures had also been characterized in detail.[52] The deposition of Ag on the platelike seeds was achieved by reducing $AgNO_3$ with ascorbic acid (AA) to generate Ag atoms. The growth was also repeated a number of times by adding more $AgNO_3$ solution. As expected, in the presence of citrate as the capping agent, the epitaxial overgrowth of Ag on the seeds generated thin plates with a similar morphology but constantly increasing edge lengths (Figure 3, B–D). After eight rounds of growth (Figure 3D), the edge length of the plates increased almost 100 times from 45 nm to 4 μm. In the presence of PVP as the capping agent, however, the growth was strongly promoted in the vertical direction, leading to an increase in thickness for the plates (Figure 3, E–G). In this case, the thickness of the plates drastically increased from 5 to 200 nm after eight rounds of growth. It should be pointed out that both lateral growth and vertical growth were observed in these two cases, so citrate and PVP did not necessarily confine the growth to a single direction while completely preventing growth in the other. However, the rate of vertical growth was reduced by eight times when PVP was replaced with citrate, while the rate of lateral growth was increased by 70 times. Overall, the vertical growth in the presence of citrate and the lateral growth in the presence of PVP were greatly reduced due to the selective binding of citrate to the {111} facets and PVP to the {100} facets, respectively. To exclusively confine the deposition of Ag on a platelike seed only to the lateral or vertical directions, the concentration of citrate or PVP might need to be further increased. Alternatively, capping agents with stronger binding

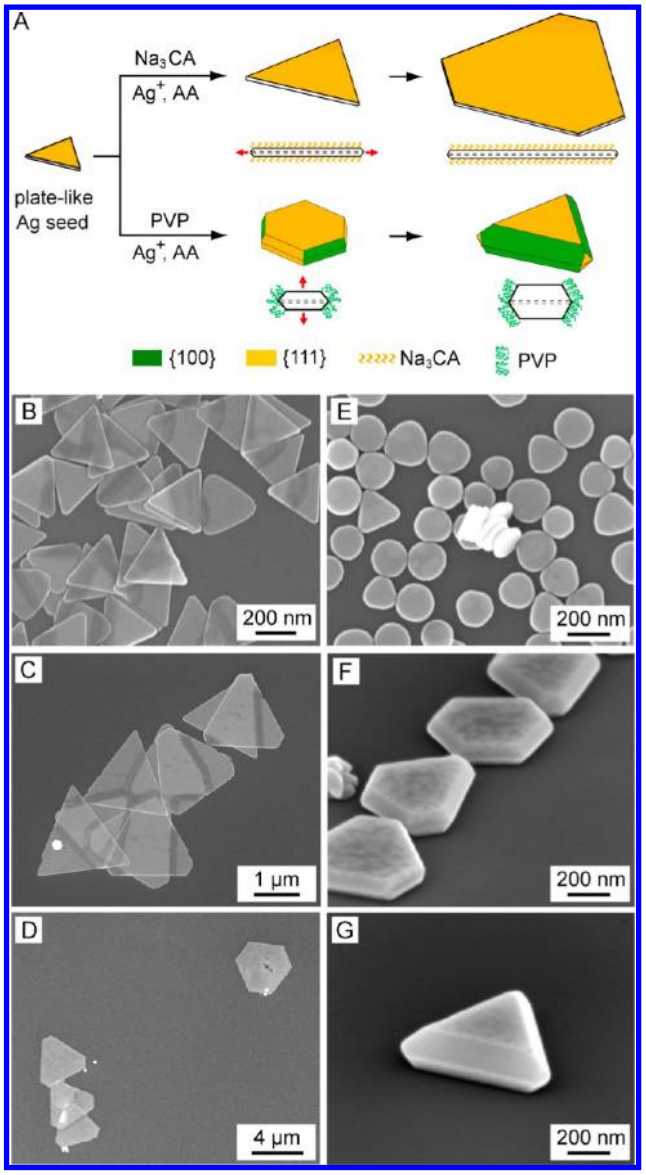

Figure 3. (A) Schematic showing the growth of a platelike Ag seed in the presence of citrate or PVP as the capping agent. For the cross-sectional side views, the major directions of growth are marked by red arrows. The stacking faults are indicated by dashed lines. (B–D) SEM images of thin Ag plates obtained by repeating the seeded growth 2, 6, and 8 times in the presence of citrate as the capping agent. Note that the length scale is considerably increased from (B) to (D). (E–G) SEM images of Ag plates obtained by repeating the seeded growth 2, 6, and 8 times in the presence of PVP as the capping agent. (Adapted with permission from ref 51, copyright 2010 Wiley-VCH).

affinities to the Ag(111) and Ag(100) surfaces have to be identified.

The difference in binding affinities for citrate and PVP toward the Ag{111} and Ag{100} facets, respectively, can be applied to different types of seeds regardless of their shapes and in the absence or presence of twin defects. It is expected that this strategy can be further extended to systems that involve other types of seeds (single-crystal or multiply twinned) and/or are made of different noble metals.

QUANTITATIVE ANALYSIS OF THE ROLE PLAYED BY PVP

Although the studies discussed in the previous two sections have demonstrated the effects of capping agents on the formation of Ag nanocrystals with different shapes, they do not offer a quantitative understanding of the role played by a facet-specific capping agent. Learning how the concentration of a capping agent affects the growth is critical to a better control of the shape evolution.

In a recent study, we reported the first quantitative analysis of the role played by PVP in a seed-mediated synthesis of Ag polyhedrons.[53] The analysis was based on a set of experiments involving the use of Ag nanocubes in ethylene glycol (EG) as the seeds, with $AgNO_3$ serving as the precursor and PVP of two molecular weights and in different initial concentrations serving as the capping agent. Figure 4A schematically illustrates how to experimentally determine the coverage density (ϕ) of PVP on the surface of Ag nanocubes. In brief, the value of ϕ could be derived by combining the results from the following two experiments. In the first experiment, we fixed the initial concentration of PVP at a relatively high level (C_1) so that there was sufficient free PVP in the solution to maintain the coverage density of PVP on the surface of cubic seeds during growth. In the initial growth stage, the cubic seeds (with an edge length of a nm) grew in size with no change in shape (Figure 4A, ***1*** to ***2***). As the reaction proceeded, the enlarged Ag(100) surface eventually caused the concentration of free PVP in the solution to drop to a critical level (C_2), at which surface passivation by PVP could no longer be maintained. At this point, the surface free energies of {100} and {111} facets became the same. Immediately passing this point, the more stable {111} facets started to appear at the corner sites, and thus slightly truncated cubes (***3*** in Figure 4A, with a size of b nm) were obtained. In the second experiment, we gradually reduced the initial concentration of PVP while other conditions were kept the same to find the critical concentration (C_2), at which the {111} facets started to appear at the very beginning of a synthesis.

Since the concentrations of free PVP and coverage densities of PVP on the Ag(100) surface should be the same for samples ***3*** and ***5***, the coverage density can then be calculated from the difference between the amounts of PVP added into these two reactions and the difference in the total surface area of Ag nanocubes for these two samples (ΔS_{Ag})

$$\phi = (C_1 - C_2)\cdot V\cdot N_A/\Delta S_{Ag} \quad (1)$$

where V is the volume of the reaction solution (0.02 L for all of our experiments) and N_A is Avogadro's number (6.02×10^{23}). The difference in surface area, ΔS_{Ag}, was calculated by multiplying the total number (1.0×10^{12}) of cubic seeds by the increase in surface area between the two samples of nanocubes, $6(b^2 - a^2)$ nm^2.

In the first set of experiments, we used Ag nanocubes with an edge length of 40 nm (a = 40 nm) and PVP with an average molecular weight of 55 000 (PVP55) as the seeds and capping agents, respectively. The 40 nm cubic seeds were prepared by quenching a polyol reaction with an ice–water bath when the major LSPR of the suspension had reached 435 nm.[54] We found that the seeds would start to show truncation at the corners at either C_1 = 1.0 mM and t = 20 min (b = 120 nm, Figure 4D) or C_2 = 0.1 mM and t = 5 min (Figure 4E).

dx.doi.org/10.1021/jp306063p | J. Phys. Chem. C 2012, 116, 21647–21656

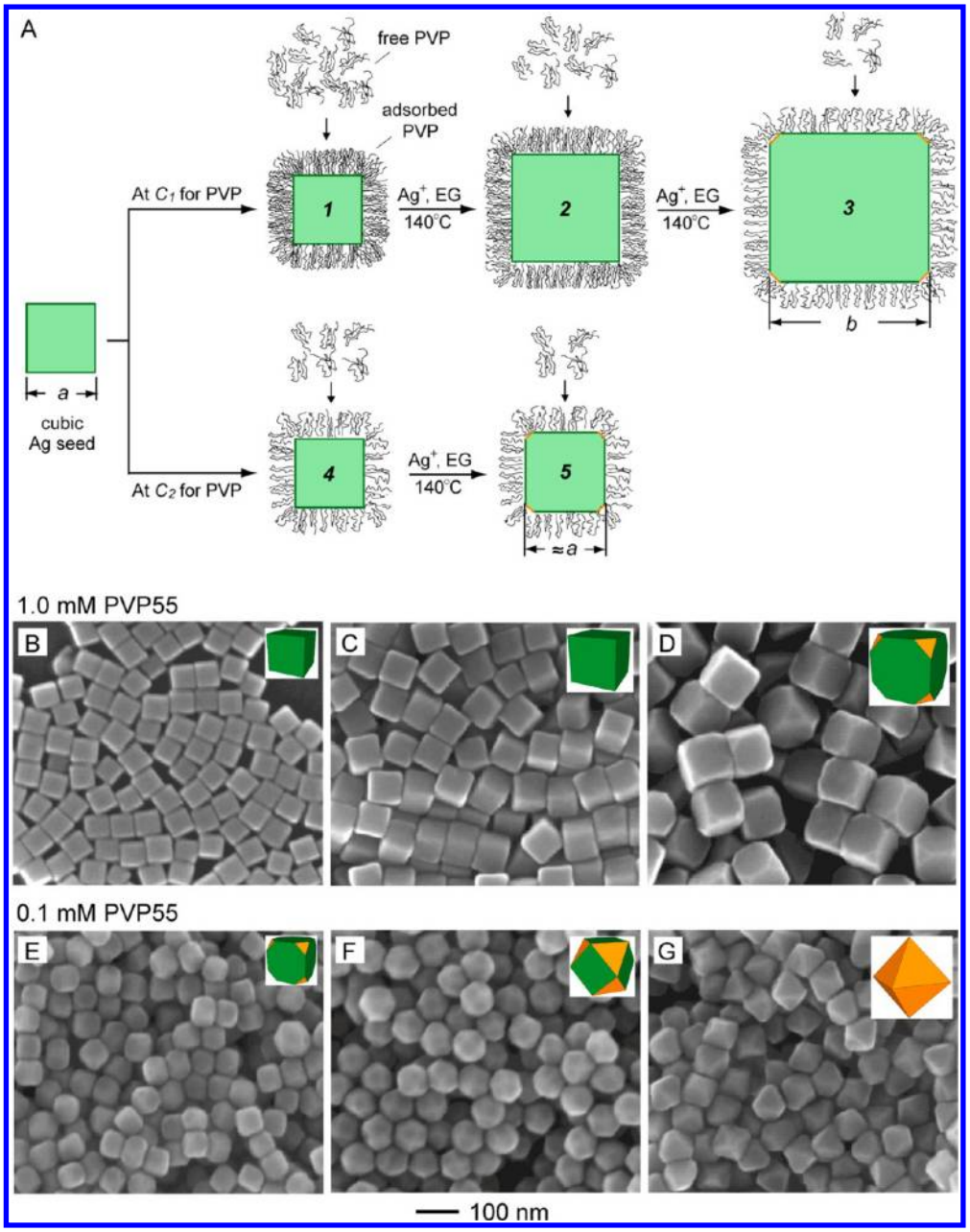

Figure 4. (A) Schematic showing the growth of a cubic Ag seed with an edge length of *a* nm in the presence of PVP at a high concentration of C_1 and a critical concentration of C_2 ($C_1 > C_2$) as the capping agent. (B–G) SEM images of Ag polyhedrons grown from 40 nm cubic seeds in the presence of (B–D) 1.0 mM and (E–G) 0.1 mM PVP55, respectively. The samples were collected from the reaction solutions at different time points: (B, E) 5 min, (C, F) 10 min, and (D, G) 20 min. The insets show the corresponding models for each type of polyhedron. (Adapted with permission from ref 53, copyright 2010 American Chemical Society).

Plugging these values into eq 1 yielded a value of ϕ = 140 repeating units per nm^2 for PVP55 and the 40 nm cubic seeds.

We also investigated the effect of PVP's molecular weight on the surface coverage density. Using the same approach for calculating the coverage density of PVP55, the value of ϕ for PVP10 ($M_W \approx 10\,000$) and 40 nm cubic seeds was found to be about 30 repeating units per nm^2. The value of ϕ for PVP10 was only about one-fourth of that for PVP55, indicating that PVP with a lower molecular weight was more effective in passivating the Ag(100) surface, likely due to more efficient adsorption and packing. Interestingly, when a monomer analog of PVP, 1-methyl-2-pyrrolidinone, was used to replace PVP10 while other reaction conditions were kept the same, the cubic seeds would grow into nearly spherical cuboctahedrons immediately after addition, which is similar to what was observed when no PVP was added into the reaction system. One possible explanation for this observation is that the lack of a polyvalency effect for the monomer analog of PVP reduced the effectiveness of binding to the Ag(100) surface.[55−57] This argument agrees well with the results obtained from the DFT calculations where the preference for PVP binding to the Ag(100) surface was found to increase exponentially with the number of repeating units.[37] We also used 100 nm cubic seeds for a similar study. The seeds were prepared using a recently reported seed-mediated growth, in which the reaction was quenched when the major LSPR of the product had reached

dx.doi.org/10.1021/jp306063p | J. Phys. Chem. C 2012, 116, 21647−21656

585 nm.[58] Remarkably, the values of ϕ for PVP55 and PVP10 adsorbed on 100 nm seeds were found to be roughly the same as the values derived for the 40 nm cubic seeds. This result suggested that ϕ has a much stronger dependence on the molecular weight of PVP than the size of the cubic seeds.

The quantitative analysis of the coverage density of PVP not only advanced our understanding of the role played by PVP but also allowed us to better control both the shape and size of Ag nanocrystals. For example, by simply controlling the initial concentration of PVP added into a reaction solution, a series of Ag polyhedrons from enlarged cubes (Figure 4C) to truncated cubes (Figure 4E), cuboctahedrons (Figure 4F), truncated octahedrons, and octahedrons (Figure 4G) could all be easily obtained from cubic seeds. In addition to shape control, the quantitative understanding of PVP also facilitated size-controlled syntheses. For example, in the presence of sufficient PVP and Ag seeds, the sizes of Ag nanocubes could be readily controlled in the range from 30 to 200 nm (Figure 5).[58] In this

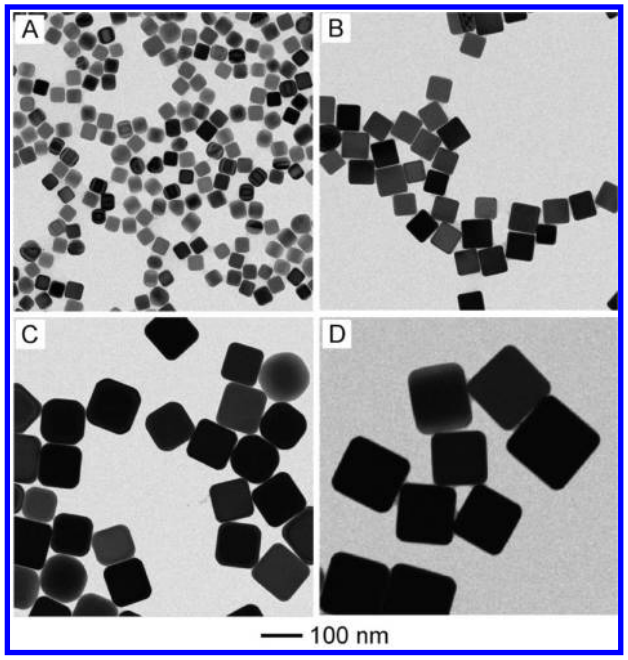

Figure 5. Size control for Ag nanocubes in a seed-mediated growth by using different amounts of $AgNO_3$ in the presence of enough PVP for capping. From (A) to (D), 10, 50, 75, and 100 μL, respectively, of $AgNO_3$ solution (282 mM, in ethylene glycol) was added to 50 μL of 29 nm single-crystal spherical Ag seeds (1.1×10^{12} particles/mL, in ethylene glycol). (Adapted with permission from ref 58, copyright 2010 American Chemical Society).

case, sufficient PVP in the reaction solution ensured an effective and constant passivation of the Ag{100} facets, making them always more stable than other facets during the growth process. As a result, the {100} facets merely increased in size as a function of the amount of precursor added into the reaction solution without the formation of {111} facets on the surface.

NANOCRYSTALS WITH HIGH-INDEX FACETS ON THE SURFACE

In the above two sections, we systematically discussed the effects of citrate and PVP on shape-controlled synthesis of Ag nanocrystals. To further evaluate their performance in passivating specific Ag facets, we recently conducted a comparative study in which we did not add additional PVP or citrate into the seed-mediated growth.[59] The synthesis involved the use of 40 nm Ag nanocubes as seeds in an aqueous system, with AA and $AgNO_3$ serving as a reductant and a salt precursor, respectively (see Figure 6A for a schematic). We

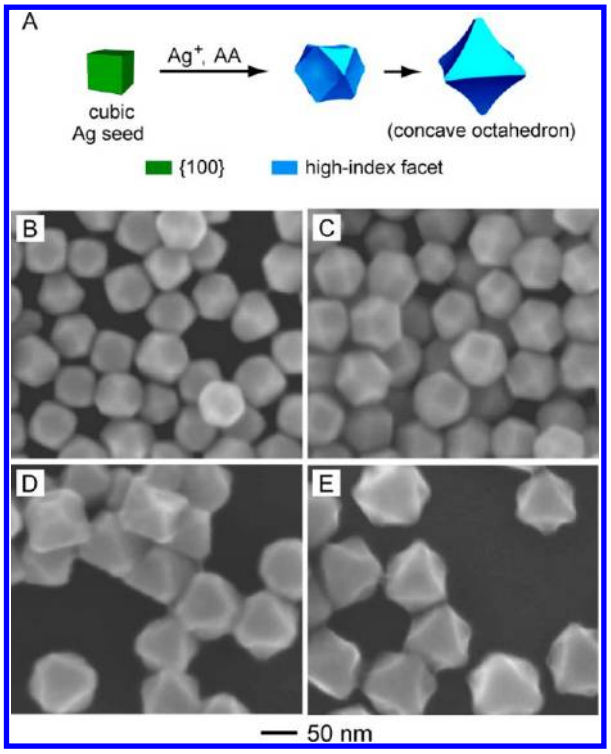

Figure 6. (A) Schematic and (B–E) SEM images showing the evolution of Ag nanocubes into concave octahedrons. In a standard synthesis, an aqueous $AgNO_3$ solution (0.2 mM) was injected into an aqueous suspension of 40 nm cubic Ag seeds (~2.0×10^9 particles/mL) and 0.3 mM ascorbic acid. The volume of $AgNO_3$ solution injected was (B) 0.8, (C) 2, (D) 4, and (E) 5 mL, respectively. (Adapted with permission from ref 59, copyright 2011 Wiley-VCH).

found that the deposition of Ag atoms ultimately led to the formation of Ag octahedrons with concave surfaces. Figure 6, B–E, shows SEM images of samples taken from the reaction solution at different stages of the synthesis. By carefully analyzing these images, we found that the growth of a cubic seed was mainly confined to the ⟨100⟩ directions, which could be attributed to the absence of a capping agent such as PVP that selectively binds to the Ag{100} facets and thus retards their growth. On the other hand, a small portion of Ag atoms were deposited along the ⟨111⟩ directions, especially at the corners and edges of a growing seed. The deposition of Ag on the {111} facets could be attributed to the absence of a capping agent such as citrate that passivates the Ag{111} facets. Taken together, the formation of concave octahedrons can be considered to arise from a combination of growth along both the ⟨100⟩ and ⟨111⟩ directions of a cubic seed. This proposed mechanism is supported by the fact that conventional Ag octahedrons with flat Ag(111) surfaces were obtained with the addition of citrate as the capping agent under similar reaction conditions.

The increase in reduction rate, in addition to the absence of capping agents, is another factor in accelerating the formation of concave structures. At a high reduction rate for $AgNO_3$, there were sufficient Ag atoms surrounding the growing seed, facilitating the deposition of Ag atoms on both the {100}

and {111} facets and thus leading to the formation of Ag octahedrons with concave surfaces. At a slow reduction rate for $AgNO_3$, however, the concentration of Ag atoms generated from the precursor was only high enough to allow deposition on the less stable {100} facets of a seed. This was confirmed by observations that concave octahedrons were only formed at relatively high concentrations of AA, and conventional octahedrons with flat surfaces were obtained when the concentration of AA was reduced (see ref 59 for a detailed discussion).

This comparative study suggested that the absence of a capping agent can lead to poor passivation of Ag surfaces. Therefore, the deposition of Ag atoms took place on various facets at different rates depending on the reaction kinetics, leading to the formation of concave structures on the surface of final products. It is expected that the curvature of the concave structure could be adjusted by controlling the reaction kinetics.

In another experiment, we introduced Cu^{2+} ions into the reaction system used for concave Ag octahedrons while the other conditions were kept the same (see Figure 7A for a schematic). To our surprise, Ag trisoctahedrons with high-index facets such as {221} and {331} were obtained. The SEM images taken from samples at different reaction stages (Figure 7, B–E) clearly show the shape evolution toward trisoctahedrons. The formation of trisoctahedrons can be illustrated by taking a cubic seed and pulling out and sharpening its eight corners. The growth of the cubic seeds occurred predominantly in the ⟨111⟩ directions, which is different from that of concave octahedrons. Although the mechanism responsible for the formation of trisoctahedrons is yet to be resolved, it might be related to the concept of underpotential deposition previously reported by Mirkin et al. for manipulating the growth of Au seeds with Ag^+ ions. The Ag^+ ions were believed to control the shape of a Au nanocrystal by depositing Ag onto specific Au facets, depending on their concentrations, preventing the deposition of Au on these facets through a galvanic replacement reaction.[60] In a similar manner, Cu^{2+} might be selectively reduced and deposited on the Ag{100} facets of a cubic seed and thus drive the deposition of Ag atoms to the poorly covered Ag{111} facets, leading to the formation of Ag trisoctahedrons.

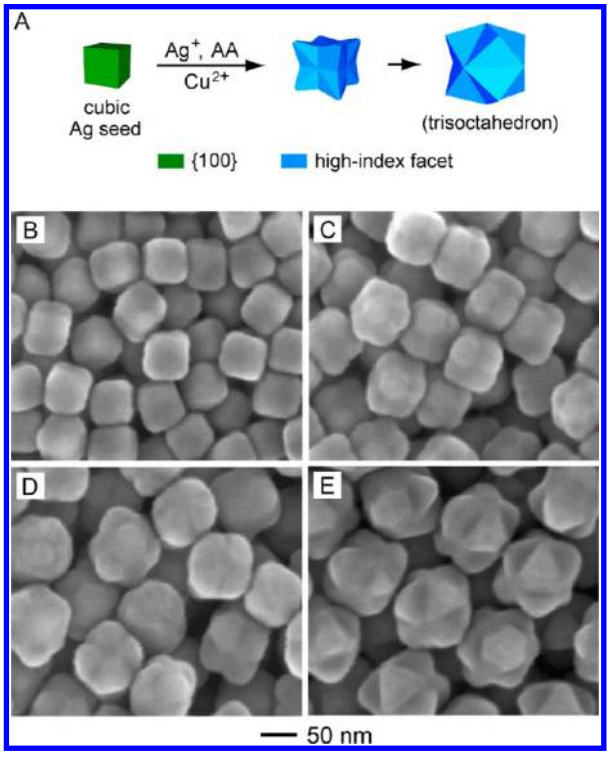

Figure 7. (A) Schematic and (B–E) SEM images showing the evolution of Ag nanocubes into trisoctahedrons. The protocol was similar to what was used for the concave Ag octahedrons (see Figure 6) except for the presence of 0.8 mM $Cu(NO_3)_2$ in the final reaction solution. The volume of $AgNO_3$ solution injected was (B) 1.5, (C) 3.5, (D) 6.5, and (E) 10 mL, respectively. (Adapted with permission from ref 59, copyright 2011 Wiley-VCH).

LSPR PROPERTIES OF THE NOVEL AG NANOCRYSTALS

The Ag nanocrystals with well-defined shapes and sizes (Figures 4–7) offer a great opportunity to investigate the dependence of their LSPR properties on both the shape and size, which is critical to evaluation of their potential applications in sensing and imaging.

Surface plasmon resonance (SPR) can be described as the resonant, collective oscillation of conduction electrons in a metallic solid stimulated by incident light.[61,62] When this oscillation is excited in a nanometer-sized particle, it is confined to the particle and thus referred to as localized SPR (LSPR). The LSPR of a Ag nanocrystal can be characterized by the extinction spectrum and has a strong dependence on both the size and shape of a particle.[6,63−67] The Ag nanocrystals with well-defined shapes (as shown in Figure 4) and controllable sizes (as shown in Figure 5) allowed us to systematically investigate the effects of shape and size on LSPR. Figure 8A compares normalized UV−vis spectra of 40 nm Ag cubic seeds and the corresponding Ag nanocrystals grown from these seeds (as shown in Figure 4, E−G). The 40 nm cubic seeds showed three LSPR peaks, including a major peak at 435 nm and two shoulder peaks at 345 and 380 nm, which are dipole resonance modes.[68] In comparison with the cubic seeds, there are only two peaks for the truncated cubes (Figure 4E), and the peak observed at ∼380 nm for the cubic seeds disappeared in the spectrum of the truncated cubes. For the spectrum of cuboctahedrons (Figure 4E), both peaks located at ∼345 and 380 nm disappeared, mainly because a cuboctahedron has higher symmetry than a cube. It is interesting that four LSPR peaks were resolved for the Ag octahedron with an average edge length of 75 nm (Figure 4G), including three weak peaks located at 350, 380, and 415 nm and one primary peak at 500 nm corresponding to one of the dipole modes.[53] Figure 8B shows normalized UV−vis spectra of Ag nanocubes with different edge lengths. As the size of the nanocubes increased from 36 to 58, 99, and 144 nm, the major LSPR peaks of these nanocubes displayed a constant red-shift from 430 to 468, 497, and 600 nm. Three LSPR peaks, which are dipole resonance modes, were present for both the 36 and 58 nm cubes. In comparison, four peaks including a small shoulder at 455 nm (a quadrupole resonance mode) can be resolved for the 99 nm cubes. These observations are consistent with the extinction spectra calculated using the discreted dipole approximation (DDA) method for Ag nanocubes with similar sizes.[68] The LSPR peaks for the 144 nm nanocubes were, however, relatively broad and thus less distinguishable, likely due to their large sizes and thus the involvement of multipode excitations.[14,68]

dx.doi.org/10.1021/jp306063p | J. Phys. Chem. C 2012, 116, 21647−21656

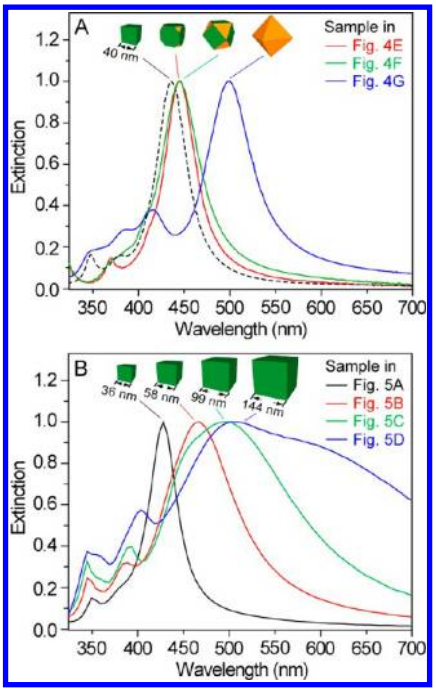

Figure 8. Normalized UV−vis spectra taken from aqueous suspensions of (A) Ag nanocrystals with different shapes and (B) Ag nanocubes with different edge lengths (as indicated in the plots and the corresponding models). In (A), the dashed curve corresponds to the UV−vis spectrum of the 40 nm Ag cubes serving as the seeds, from which the other Ag nanocrystals were grown. (Adapted with permissions from refs 53 and 58, copyrights 2012 and 2010 American Chemical Society).

SUMMARY AND OUTLOOK

All the way through this article, we have discussed how a facet-specific capping agent can be used to control the shape evolution of Ag nanocrystals in a seed-mediated synthesis. Specifically, citrate and PVP were found to selectively bind to the {111} and {100} facets of Ag, respectively, making them more stable than other facets and thus favoring the formation of Ag nanocrystals with {111} or {100} facets exposed on the surface. In comparison with other methods, the use of a facet-specific capping agent seems to be more flexible, versatile, and predictable. The resultant Ag nanocrystals simply take a specific shape with the expected facets depending on the type and concentration of a capping agent added into the reaction solution. For example, Ag octahedrons enclosed by {111} facets could be obtained from spherical or cubic Ag seeds in the presence of citrate as a capping agent, while Ag cubes enclosed by {100} facets were obtained from the same seeds when PVP was employed as a capping agent. In a similar manner, a series of Ag nanocrystals with controlled sizes and novel shapes were obtained from different types of seeds. We have also quantified the coverage density of PVP with different molecular weights on the Ag(100) surface. With this quantitive data, syntheses of Ag polyhedrons with different sizes and proportions of {100} to {111} facets become feasible and controllable. It is still necessary to find effective approaches to quantitatively analyze the roles played by other capping agents. It should be pointed out that the facet-specific capping of citrate and PVP is not limited to Ag. At least, they have similar impacts on Pd.[69,70] In addition to citrate and PVP, several other capping agents have also been reported in the literature. For example, Br^- ions have been identified with an ability to selectively cap the {100} facets of Ag, Au, Pd, and Pt to induce the formation of nanocubes, rectangular nanobars, and octagonal nanorods.[24] Formaldehyde has been shown to selectively bind to the {111} facets of Pd, thus favoring the formation of Pd decahedrons, octahedrons, and nanoplates.[71,72] An extension of the concept of facet-specific capping to other noble metals (e.g., Au, Pt, Pd, and Rh) has enabled and will enable us to process these metals into nanocrystals with various controllable shapes. Meanwhile, screening new capping agents that can selectively cap a specific set of facets, especially the high-index facets,[73] is also an interesting issue that deserves thorough exploration in the future.

AUTHOR INFORMATION

Corresponding Author

*E-mail: younan.xia@bme.gatech.edu.

Notes

The authors declare no competing financial interest.

Biographies

Younan Xia is the Brock Family Chair and GRA Eminent Scholar in Nanomedicine in the Wallace H. Coulter Department of Biomedical Engineering, with joint appointment in School of Chemistry and Biochemistry and School of Chemical and Biomolecular Engineering at Georgia Institute of Technology. He received a B.S. in Chemical Physics from the University of Science and Technology of China in 1987, an M.S. in Inorganic Chemistry from the University of Pennsylvania (with Prof. Alan G. MacDiarmid) in 1993, and a Ph.D in Physical Chemistry from Harvard University (with Prof. George M. Whitesides) in 1996. He started as an Assistant Professor of Chemistry at the University of Washington (Seattle) in 1997 and was promoted to Associate Professor and Professor in 2002 and 2004, respectively. From 2007 to 2011, he was the James M. McKelvey Professor for Advanced Materials in the Department of Biomedical Engineering at Washington University in St. Louis, and his group moved to Georgia Institute of Technology at the beginning of 2012. His current research interests include nanomaterials, biomaterials, nanomedicine, electrospinning, and colloidal science.

Xiaohu Xia was born in Anhui, China, 1984. He received his B.S. in Biotechnology and Ph.D. in Biochemistry and Molecular Biology from Xiamen University in 2006 and 2011, respectively. He worked as a visiting graduate student at Washington University in St. Louis from October 2009 through November 2011. He is currently a postdoctoral fellow in the Xia group at Georgia Institute of Technology. His research interests include the design and synthesis of novel nanostructures and their use in catalytic and biomedical applications.

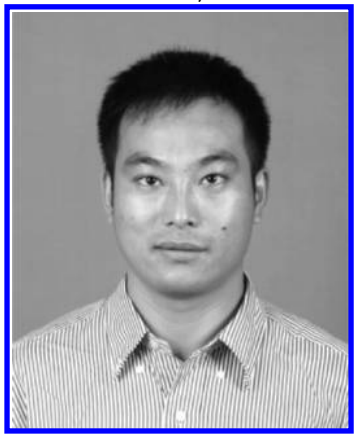

Jie Zeng was born in Henan, China, in 1980. He studied Applied Chemistry at the University of Science and Technology of China (B.S., 2002) and received his Ph.D. in Condensed Matter Physics under the tutelage of Prof. Jianguo Hou (2007). He worked in the Xia group as a postdoctoral fellow at Washington University in St. Louis from 2008 to 2011 and was promoted to Research Assistant Professor in 2011. In 2012, he moved back to the University of Science and Technology of China to take the position of Qianren Professor for Chemistry in Hefei National Laboratory for Physical Sciences at the Microscale. His research interests include synthesis and utilization of novel nanostructures for plasmonics and catalysis.

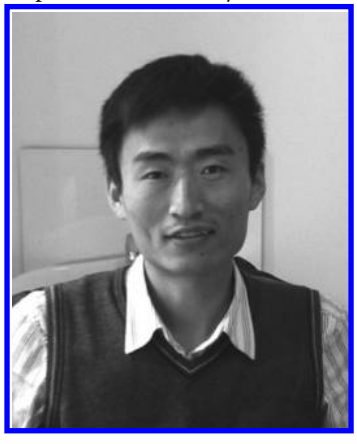

Qiang Zhang received his B.S. in Materials Physics and Ph.D. in Biochemistry and Molecular Biology from the University of Science and Technology of China in 2005 and 2011, respectively. He worked as a jointly supervised student in the Xia group from October 2008 to September 2010. He is currently an Associate Professor in Biomedical Engineering at the East China Normal University. His research interests include syntheses of noble-metal nanostructures and their applications in catalysis, optical sensing, and biomedicine.

Christine Moran received her B.S. in Bioengineering from Rice University in 2009 and her M.S. in Biomedical Engineering from Washington University in St. Louis in 2011. She is currently pursuing her Ph.D. in Biomedical Engineering at Georgia Institute of Technology in the Xia group. Her research interests revolve around the biomedical applications of SERS and novel polymeric nanocarriers.

■ ACKNOWLEDGMENTS

The work was partially supported by the NSF (DMR, 1104614 and 1215034), the NIH (NCI, R01 CA13852701), an NIH Director's Pioneer Award (DP1 OD000798), and startup funds from Georgia Institute of Technology. As jointly supervised Ph.D. students from Xiamen University and the University of Science and Technology of China, respectively, X.X. and Q.Z. were also partially supported by Fellowships from the China Scholarship Council.

■ REFERENCES

(1) Kelly, K. L.; Coronado, E.; Zhao, L. L.; Schatz, G. C. *J. Phys. Chem. B* **2003**, *107*, 668−677.
(2) El-Sayed, M. A. *Acc. Chem. Res.* **2001**, *34*, 257−264.
(3) Evanoff, D. D.; Chumanov, G. *Chem. Phys. Chem.* **2005**, *6*, 1221−1231.
(4) Nie, S.; Emory, S. R. *Science* **1997**, *275*, 1102−1106.
(5) McFarland, A. D.; Van Duyne, R. P. *Nano Lett.* **2003**, *3*, 7426−7433.
(6) Wiley, B. J.; Im, S. H.; Li, Z. Y.; McLellan, A. S.; Xia, Y. *J. Phys. Chem. B* **2006**, *110*, 15666−15675.
(7) He, J.; Ichinose, I.; Kunitake, T.; Nakao, A.; Shiraishi, Y.; Toshima, N. *J. Am. Chem. Soc.* **2003**, *125*, 11034−11040.
(8) Wu, Y.; Li, Y.; Ong, B. S. *J. Am. Chem. Soc.* **2007**, *129*, 1862−1863.
(9) Peng, H. I.; Strohsahl, C. M.; Leach, K. E.; Krauss, T. D.; Miller, B. L. *ACS Nano* **2009**, *3*, 2265−2273.
(10) Rycenga, M.; Cobley, C. M.; Zeng, J.; Li, W.; Moran, C. H.; Zhang, Q.; Qin, D.; Xia, Y. *Chem. Rev.* **2011**, *111*, 3669−3712.
(11) Jin, R.; Cao, Y.; Mirkin, C. A.; Kelly, K. L.; Schatz, G. C.; Zheng, J. G. *Science* **2001**, *294*, 1901−1903.
(12) Jana, N. R.; Gearheart, L.; Murphy, C. J. *Chem. Commun.* **2001**, 617−618.
(13) Sun, Y.; Xia, Y. *Science* **2002**, *298*, 2176−2179.

(14) Tao, A. R.; Sinsermsuksakul, P.; Yang, P. *Angew. Chem., Int. Ed.* **2006**, *45*, 4597−4601.
(15) Pietrobon, B.; Kitaev, V. *Chem. Mater.* **2008**, *20*, 5186−5190.
(16) Zhang, J.; Li, S.; Wu, J.; Schatz, G. C.; Mirkin, C. A. *Angew. Chem., Int. Ed.* **2009**, *48*, 7787−7791.
(17) Ozin, G. A. *Catal. Rev. Sci. Eng.* **1977**, *16*, 191−289.
(18) Roberts, M. W. *Surf. Sci.* **1994**, *299*, 769.
(19) Chen, Q.; Richardson, N. V. *Prog. Surf. Sci.* **2003**, *73*, 59−77.
(20) Harris, P. J. F. *Nature* **1986**, *323*, 792−794.
(21) Wang, Z. L. *J. Phys. Chem. B* **2000**, *104*, 1153−1175.
(22) Zhang, J. M.; Ma, F.; Xu, K. W. *Appl. Surf. Sci.* **2004**, *229*, 34−42.
(23) Frenken, J. W. M.; Stoltze, P. *Phys. Rev .Lett.* **1999**, *82*, 3500−3503.
(24) Xia, Y.; Xiong, Y.; Lim, B.; Skrabalak, S. E. *Angew. Chem., Int. Ed.* **2009**, *48*, 60−103.
(25) Vitos, L.; Ruban, A. V.; Skriver, H. L.; Kollar, J. *Surf. Sci.* **1998**, *411*, 186−202.
(26) Tao, A. R.; Habas, S.; Yang, P. *Small* **2008**, *4*, 310−325.
(27) Vitos, L.; Ruban, A. V.; Skriver, H. L.; Kollar, J. *Surf. Sci.* **1998**, *411*, 186−202.
(28) Sun, Y.; Mayers, B.; Herricks, T.; Xia, Y. *Nano Lett.* **2003**, *3*, 955−960.
(29) Wiley, B. J.; Chen, Y.; McLellan, J. M.; Xiong, Y.; Li, Z. Y.; Ginger, D.; Xia, Y. *Nano Lett.* **2007**, *7*, 1032−1036.
(30) Jin, R. C.; Cao, Y. C.; Hao, E.; Metraux, G. S.; Schatz, G. C.; Mirkin, C. A. *Nature* **2003**, *425*, 487−490.
(31) Kilin, D. S.; Prezhdo, O. V.; Xia, Y. *Chem. Phys. Lett.* **2008**, *458*, 113−116.
(32) Mahmoud, M. A.; Tabor, C. E.; El-Sayed, M. A. *J. Phys. Chem. C* **2009**, *113*, 5493−5501.
(33) Moran, C. H.; Rycenga, M.; Zhang, Q.; Xia, Y. *J. Phys. Chem. C* **2011**, *115*, 21852−21857.
(34) Bonet, F.; Tekaia-Elhsissen, K.; Sarathy, K. V. *Bull. Mater. Sci.* **2000**, *23*, 165−168.
(35) Huang, H. H.; Ni, X. P.; Loy, G. L.; Chew, C. H.; Tan, K. L.; Loh, F. C.; Deng, J. F.; Gu, G. Q. *Langmuir* **1996**, *12*, 909−912.
(36) Gao, Y.; Jiang, P.; Liu, D. F.; Yuan, H. J.; Yan, X. Q.; Zhou, Z. P.; Wang, J. X.; Song, L.; Liu, L. F.; Zhou, W. Y.; Wang, G.; Wang, C. Y.; Xie, S. S. *J. Phys. Chem. B* **2004**, *108*, 12877−12881.
(37) Al-Saidi, W. A.; Feng, H.; Fichthorn, K. A. *Nano Lett.* **2012**, *12*, 997−1001.
(38) Jana, N. R.; Gearheart, L.; Murphy, C. J. *J. Phys. Chem. B* **2001**, *105*, 4065−4067.
(39) Sun, Y.; Gates, B.; Mayers, B.; Xia, Y. *Nano Lett.* **2002**, *2*, 165−168.
(40) Habas, S. E.; Lee, H.; Radmilovic, V.; Somorjai, G. A.; Yang, P. *Nat. Mater.* **2007**, *6*, 692−697.
(41) Fan, F. R.; Liu, D. Y.; Wu, Y.; Duan, S.; Xie, Z. X.; Jiang, Z. Y.; Tian, Z. Q. *J. Am. Chem. Soc.* **2008**, *130*, 6949−6951.
(42) Xue, C.; Millstone, J. E.; Li, S.; Mirkin, C. A. *Angew. Chem., Int. Ed.* **2007**, *46*, 8436−8439.
(43) Chen, Y.-H.; Hung, H.-H.; Huang, M. H. *J. Am. Chem. Soc.* **2009**, *131*, 9114−9121.
(44) Zeng, J.; Zheng, Y.; Rycenga, M.; Tao, J.; Li, Z. Y.; Zhang, Q.; Zhu, Y.; Xia, Y. *J. Am. Chem. Soc.* **2010**, *132*, 8552−8553.
(45) Pastoriza-Santos, I.; Liz-Marzan, L. M. *Nano Lett.* **2002**, *2*, 903−905.
(46) Chen, S. H.; Carroll, D. L. *Nano Lett.* **2002**, *2*, 1003−1007.
(47) Bastys, V.; Pastoriza-Santos, I.; Rodriguez-Gonzalez, B.; Vaisnoras, R.; Liz-Marzan, L. M. *Adv. Funct. Mater.* **2006**, *16*, 766−773.
(48) Maillard, M.; Huang, P. R.; Brus, L. *Nano Lett.* **2003**, *3*, 1611−1615.
(49) Washio, I.; Xiong, Y.; Yin, Y.; Xia, Y. *Adv. Mater.* **2006**, *18*, 1745−1749.
(50) Zhang, Q.; Hu, Y.; Guo, S.; Goebl, H.; Yin, Y. *Nano Lett.* **2010**, *10*, 5037−5042.
(51) Zeng, J.; Xia, X.; Rycenga, M.; Henneghan, P.; Li, Q.; Xia, Y. *Angew. Chem., Int. Ed.* **2011**, *50*, 244−249.
(52) Zeng, J.; Roberts, S.; Xia, Y. *Chem.—Eur. J.* **2010**, *16*, 12559−12563.
(53) Xia, X.; Zeng, J.; Oetjen, L. K.; Li, Q.; Xia, Y. *J. Am. Chem. Soc.* **2012**, *134*, 1793−1801.
(54) Zhang, Q; Li, W.; Wen, L. P.; Chen, J.; Xia, Y. *Chem.—Eur. J.* **2010**, *16*, 10234−10239.
(55) Joralemon, M. J.; O'Reilly, R. K.; Hawker, C. J.; Wooley, K. L. *J. Am. Chem. Soc.* **2005**, *127*, 16892−16899.
(56) Tassin, J. F.; Siemens, R. L.; Tang, W. T.; Hadziioannou, G.; Swalen, J. D.; Smith, B. A. *J. Phys. Chem. B* **1989**, *93*, 2106−2111.
(57) Kim, S.; Bawendi, M. G. *J. Am. Chem. Soc.* **2003**, *125*, 14652−14653.
(58) Zhang, Q.; Li, W.; Moran, C.; Zeng, J.; Chen, J.; Wen, L. P.; Xia, Y. *J. Am. Chem. Soc.* **2010**, *132*, 11372−11378.
(59) Xia, X.; Zeng, J.; McDearmon, B.; Zheng, Y.; Li, Q.; Xia, Y. *Angew. Chem., Int. Ed.* **2011**, *50*, 12542−12546.
(60) Personick, M. L.; Langille, M. R.; Zhang, J.; Mirkin, C. A. *Nano Lett.* **2011**, *11*, 3394−3398.
(61) Jenson, T. R.; Malinsky, M. D.; Haynes, C. L.; Van Duyne, R. P. *J. Phys. Chem. B* **2000**, *104*, 10549−10556.
(62) Link, S.; El-Sayed, M. A. *Annu. Rev. Phys. Chem.* **2003**, *54*, 331−366.
(63) Noginov, M. A.; Zhu, G.; Bahoura, M.; Adegoke, J.; Small, C.; Ritzo, B. A.; Drachev, V. P.; Shalaev, V. M. *Appl. Phys. B: Laser Opt.* **2007**, *85*, 455−460.
(64) Kreibig, U.; Vollmer, M. *Optical Properties of Metal Clusters*; Springer-Verlag: Heidelberg, Germany, 1995; Vol. 25.
(65) Amendola, V.; Bakr, O. M.; Stellacci, F. *Plasmonics* **2010**, *5*, 85−97.
(66) Taleb, A.; Petit, C.; Pileni, M. P. *J. Phys. Chem. B* **1998**, *102*, 2214−2220.
(67) Cobley, C. M.; Skrabalak, S. E.; Campbell, D. J.; Xia, Y. *Plasmonics* **2009**, *4*, 171−179.
(68) Zhou, F.; Li, Z. Y.; Liu, Y.; Xia, Y. *J. Phys. Chem. C* **2008**, *112*, 20233−20240.
(69) Xiong, Y.; Chen, J.; Wiley, B.; Xia, Y.; Yin, Y.; Li, Z.-Y. *Nano Lett.* **2005**, *5*, 1237−1242.
(70) Lim, B.; Xiong, Y.; Xia, Y. *Angew. Chem., Int. Ed.* **2007**, *46*, 9279−9282.
(71) Carneiro, J.; Cruz, M. *J. Phys. Chem. A* **2008**, *112*, 8929−8937.
(72) Niu, Z.; Peng, Q.; Gong, M.; Rong, H.; Li, Y. *Angew. Chem., Int. Ed.* **2011**, *50*, 6315−6319.
(73) Zhang, H.; Jin, M.; Xia, Y. *Angew. Chem., Int. Ed.* **2012**, *51*, 7656−7673.